CYBERNETICS AND PHYSICS, VOL. 1, NO. 2, 2012 , 89–95

# STUDY OF THE FOUCAULT PENDULUM WITHIN THE GEOMETRIC CONTROL THEORY PERSPECTIVE

**Alfonso Anzaldo-Meneses**
Basic Sciences Department
UAM-Azcapotzalco
Av. San Pablo 100, Azcapotzalco
02200 México D.F.
answald@ymail.com

**Felipe Monroy-Pérez**
Basic Sciences Department
UAM-Azcapotzalco
Av. San Pablo 100, Azcapotzalco
02200 México D.F.
fmp@correo.azc.uam.mx

**Abstract**
In this paper we study the classical Foucault pendulum, indisputable demonstration of the Earth's rotation movement, through the formalism of geometric control theory. The Pontryagin Maximum Principle is applied for deriving some geometric properties of trajectories in the particular case of small oscillations. A link between the geometry of trajectories and the well known Hopf fibration is established.

**Key words**
Foucault pendulum, geometric control, Pontryagin principle.

## 1 Introduction

In this paper we approach the system that models the experiment of the Foucault pendulum, through the framework of the geometric optimal control theory. We restrict ourselves to small oscillations and to the symmetric case. We write the equations as an optimal control system on a three dimensional manifold and apply the Pontryagin Maximum Principle for deriving some geometric properties of the solutions.

Geometric non-linear control theory merges differential geometric techniques with the analysis of different aspects of non-linear control systems, including equilibria, stabilization, and optimal control problems. The foundations of the theory goes back to the early seventies with the pioneering papers [Lobry, 1970], [Brockett, 1972], and [Jurdjevic and Sussmann, 1972], among others.

The theory has been especially successful in applications to certain problems in geometric mechanics [Bullo and Lewis, 2004] and robotics [Murray, Zexiang and Sastry, 1994]. There is an extensive literature presenting the general theory of geometric non-linear control systems, we refer the reader to the volume [Jurdjevic, 1997] and the recent book [Agrachev and Sachkov, 2004].

An optimal control problem on an path-connected a smooth manifold is given by two ingredients: a non-linear control system and a functional defined in the space of solutions of the system. In this generality the problem consists in finding, among the solutions of the control system, the one that optimizes the functional.

Geometric optimal control for non-linear systems finds its origin in the Pontryagin Maximum Principle (PMP), originally published in the book [Pontryagin em et al., 1962]. This important result and its subsequent generalizations provide natural extensions of the necessary conditions for optimality stated in the classical calculus of variations, see for instance [Giaquinta and Hildebrandt, 1996], and has recently lead to new geometry that goes in the literature under the name of Sub-Riemannian or Carnot-Caratheodory geometry. Generally speaking a sub-Riemannian structure on a manifold $\mathcal{M}$ is determined by a completely non-integrable (non-holonomic), distribution of vector fields, for details see for instance the excellent survey [Vershik and Gershkovich, 1991], the volume [Montgomery, 2002], and the recent book [Calin and Chang, 2009].

Apart from this introduction this paper contains six sections, in Section 2 we describe the optimal control problem for a system defined by means of a completely non-integrable distribution of smooth vector fields, framework under which the system corresponding to the Foucault pendulum shall be approached, in Section 3 we present the standard mathematical model of the pendulum. In Section 4, under certain considerations for small oscillations, we formulate the Foucault pendulum as an optimal control approach an a smooth manifold, for which we apply the PMP for deriving geometric properties of solutions. In Section 5 we establish a natural connection of the trajectories of the problem to the well known Hopf fibration. Sec-

tion 6 includes some technical details on the Foucault pendulum that is in the process of being installed at the Universidad Autónoma Metropolitana-Azcapotzalco in México City. At the end, in Section 7 we derive some conclusions and discuss further research perspectives.

## 2 The Optimal Control Theory Viewpoint

Let $\mathcal{M}$ be a $n$-dimensional path-connected smooth manifold $\mathcal{M}$, and let $\Delta \subset T\mathcal{M}$ be a rank $k < n$ distribution of smooth vector fields on $\mathcal{M}$. The iteration of the Lie bracket of the vector fields in $\Delta$ yields the following flag of modules of vector fields:

$$\Delta^1 \subset \Delta^2 \subset \cdots \subset \Delta^l \cdots \subset T\mathcal{M},$$

where $\Delta^1 = \Delta$ and $\Delta^{i+1} = \Delta^i + [\Delta, \Delta^i]$.

The distribution is said to be *bracket generating*, if for each $m \in \mathcal{M}$, there exist a positive integer $\ell$ for which $\Delta^\ell_m = T_m\mathcal{M}$. The *growth vector* of $\Delta$ at $m$ is defined as $(n_1, \ldots, n_l)$, where $n_j(m) = \dim(\Delta^j_m)$, the distribution is said to be *regular* if the growth vector is independent of the base point.

A regular, bracket generating distribution $\Delta$ generated by basis of vector fields $\{X_1, \ldots, X_k\}$ determines intrinsically a non-linear control system without drift as we now explain. An absolutely continuous curve $t \mapsto q(t)$, $t \in [0, \tau_q]$ is said to be $\Delta-$admissible is $\dot{q}(t) \in \Delta(q(t))$, for almost all $t \in [0, \tau_q]$, this admissibility condition implies that for almost any $t \in [0, \tau_q]$ there exists a bounded and measurable vector function $u(t) = (u_1(t), \ldots, u_k(t))$, such that

$$\dot{q} = u_1 X_1(q) + \cdots + u_k X_k(q). \tag{1}$$

Under these circumstances, equation (1) defines a non-linear control system on $\mathcal{M}$ with the $u(t)$ playing the role of the control parameter, the set of all admissible controls is denoted as $\mathcal{U}$.

In summary, a $\Delta-$admissible curve $t \mapsto q(t)$, $t \in [0, \tau_q]$, comes together with a control parameter $u(t) \in \mathcal{U}$ and the pair $(q(t), u(t))$ yields an admissible trajectory of the control system (1) according to the ordinary definition of the non-linear control theory, moreover standard results of the theory guarantee the existence of solutions for any given initial condition, see for instance [Young, 1969].

The system (1) is said to be *controllable*, if for any pair of points $m_i, m_f \in \mathcal{M}$ one can find and admissible trajectory $(q(t), u(t))$, $t \in [0, \tau_q]$ satisfying $q(0) = m_i$ and $q(\tau_q) = m_f$. It is known that for a regular, bracket generating distribution $\Delta$ the system (1) is controllable.

The space $\mathcal{A}$ of all admissible trajectories of (1) has the structure of Sobolev space and for any, regular enough, function $c : \mathcal{A} \to \mathbb{R}$, one can consider the functional

$$\mathcal{E} = \int_0^{\tau_q} c(q(t), \mathbf{u}(t))\, dt, \tag{2}$$

Assembling all these elements together we end up with an optimal control problem on $\mathcal{M}$ consisting in finding, among the solutions of (1) the one that minimizes (2).

Necessary conditions for admissible optimal trajectories of the above optimal control problem are given by the well known Pontryagin Maximum Principle PMP, originally presented in the classical book of L.D. Pontryagin and collaborators [Pontryagin em et al., 1962]. Several versions appear interspersed in the literature, we follow the one exposed in V. Jurdjevic's book [Jurdjevic, 1997].

The cotangent bundle $T^*\mathcal{M}$ is a symplectic manifold with canonical symplectic form $\Omega$, that allows to associate to each smooth function $\mathcal{H} : T^*\mathcal{M} \to \mathbb{R}$, a Hamiltonian vector field $\vec{H}$, according to the expression $dH_\xi(v) = \Omega(v, \vec{\mathcal{H}}(\xi))$, where $v \in T_\xi T^*\mathcal{M}$ and $\xi \in T^*\mathcal{M}$. For then the Hamiltonian flow $t \mapsto \xi(t) = (q(t), p(t))$ obeys the so-called Hamilton equations

$$\frac{dq}{dt} = \nabla_p \mathcal{H} \tag{3}$$

$$\frac{dp}{dt} = -\nabla_q \mathcal{H}, \tag{4}$$

If $H_i(\xi) = \xi(X_i)$, $i = 1, \ldots, k$, then for system (1) one can define the following Hamiltonian function

$$\mathcal{H}_{\lambda_0, u}(\xi) = \lambda_0 c(q, u) + \sum_{i=1}^{k} u_i(t) H_i(\xi), \tag{5}$$

the multiplier $\lambda_0$ is customary normalized for taking values 1 (normal) or 0 (abnormal), we consider only the case $\lambda_0 = 1$. The PMP establishes then the following necessary condition for the optimal controls.

**Theorem 2.1.** *If $(q(t), \mathbf{u}(t))$, $t \in [0, \tau_q]$ is an optimal trajectory then there is an integral curve $t \mapsto \xi(t)$, $t \in [0, \tau_q]$ of the Hamiltonian vector field $\vec{\mathcal{H}}_{\mathbf{u}}$ such that*

1. *$\xi(t) \neq 0$ and $q(t)$ is the projection of $\xi(t)$*
2. *$\mathcal{H}_{\mathbf{u}}(\xi) = \sup_{u \in \mathcal{U}} \mathcal{H}_u$*

Applying this theorem one can derive necessary condition for optimal trajectories by analyzing the geometry of the corresponding extremal curves that can be parameterized as $\xi = (H_1, \ldots, H_k)$.

## 3 The Standard Model for the Foucault Pendulum

We take and inertial frame with coordinates $(X, Y, Z)$, and a pendulum of length $\ell$ and point mass $m$, oscillating taking into consideration Earth's rotation movement. The angular velocity of the rotation is denoted as $\vec{\omega}$, and the mass' position is measured from a fixed coordinate system with origin located at latitude $\alpha$ and coordinates $(x_1, x_2, x_3)$, the $x_1$ direction on a meridian great circle in north-south sense, the $x_2$ direction on a latitude circle in west-east sense and the $x_3$ direction

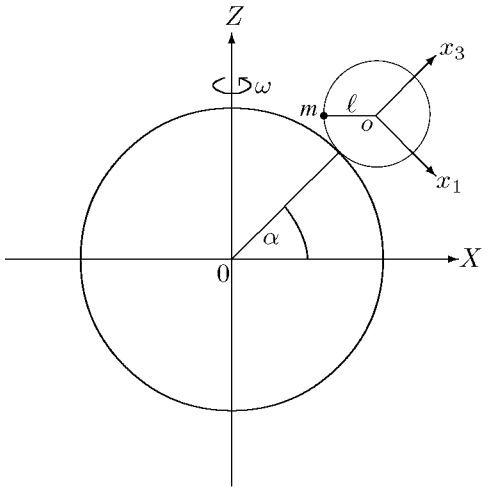


Figure 1. Pendulum at geographic latitude $\alpha$.

perpendicular to the tangent plane at the intersection of both circles, see Figure 1.

A vector $\vec{r}$ in the non-inertial system on Earth's surface behaves as

$$\frac{d\vec{r}}{dt} = \dot{\vec{r}} + \vec{\omega} \times \vec{r},$$

where $\dot{\vec{r}} = (\dot{x}, \dot{x_2}, \dot{x_3})$ and $\vec{\omega} = (-\omega\cos\alpha, 0, \omega\sin\alpha)$, with $\omega \approx 10^{-4}$ sec$^{-1}$. The kinetic energy is given as follows

$$\frac{m}{2}\left|\frac{d\vec{r}}{dt}\right|^2 = \frac{m}{2}(|\dot{\vec{r}}|^2 + |\vec{\omega} \times \vec{r}|^2 + 2\dot{\vec{r}} \cdot (\vec{\omega} \times \vec{r}) ).$$

The second term leads to a centrifugal force perpendicular to the rotation axis and can be disregarded, for the third term we observe that

$$\begin{aligned}\dot{\vec{r}} \cdot (\vec{\omega} \times \vec{r}) &= \vec{\omega} \cdot (\vec{r} \times \dot{\vec{r}}) \\ &= \omega_{x_1}(x_2\dot{x_3} - x_3\dot{x_2}) + \omega_{x_2}(x_3\dot{x_1} - x_1\dot{x_3}) \\ &+\omega_{x_3}(x_1\dot{x_2} - x_2\dot{x_1}),\end{aligned}$$

finally we also have to take into account the following holonomic constraint

$$\delta x_1^2 + x_2^2 + x_3^2 - \ell^2 = 0, \tag{6}$$

where $\delta$ is a dimensionless asymmetry parameter due to different moments of inertia or some other asymmetries of the experiment, for details see [Anzaldo-Menenses and Monroy-Pérez, 2010].

Taking all these constraints into consideration, we have that the complete functional is written as follow:

$$\begin{aligned}\mathcal{S} = \int \Big( &(\frac{m}{2}(\dot{x_1}^2 + \dot{x_2}^2 + \dot{x_3}^2 - 2gx_3) \\ &+ \lambda_0(\delta x_1^2 + x_2^2 + x_3^2 - \ell^2) \\ &+ \lambda_1(\dot{\xi}_1 + x_2\dot{x_3} - x_3\dot{x_2}) \\ &+ \lambda_2(\dot{\xi}_2 + x_3\dot{x_1} - x_1\dot{x_3}) \\ &+ \lambda_3(\dot{\xi}_3 + x_1\dot{x_2} - x_2\dot{x_1})\Big)\, dt,\end{aligned}$$

where $\lambda_0$ Lagrange parameter and $\lambda_1 = -m\omega\cos\alpha$, $\lambda_2 = 0$ and $\lambda_3 = m\omega\sin\alpha$, (the last differentials do not alter the Euler-Lagrange equations for $\vec{r}$). The $\lambda_i$ can be taken as the Lagrange parameters associated with the nonholonomic constraints

$$\omega_1 = d\xi_1 + x_2dx_3 - x_3dx_2 = 0, \tag{7}$$
$$\omega_2 = d\xi_2 + x_3dx_1 - x_1dx_3 = 0, \tag{8}$$
$$\omega_3 = d\xi_3 + x_1dx_2 - x_2dx_1 = 0, \tag{9}$$

which is tantamount of saying that the $\omega_i's$ are constants, since the $\xi_i's$ are cyclic variables.

## 4 Optimal Control Viewpoint for the Foucault Pendulum

We consider the Lagrangian

$$\begin{aligned}L_0 = &\frac{m}{2}(\dot{x}_1^2 + \dot{x}_2^2 + \dot{x}_3^2) - mgx_3 \\ &+ \lambda_1(\dot{\xi}_1?x_2\dot{x}_3 + x_3\dot{x}_2) \\ &+ \lambda_2(\dot{\xi}_2?x_3\dot{x}_1 + x_1\dot{x}_3) \\ &+ \lambda_3(\dot{\xi}_3?x_1\dot{x}_2 + x_2\dot{x}_3),\end{aligned}$$

subject to constraint (6). The last three terms of the Lagrangian result from the fact that the pendulum is in a non-inertial coordinates system. Equivalently, we can take the Lagrangian

$$L = \frac{m}{2}(\dot{x}_1^2 + \dot{x}_2^2 + \dot{x}_3^2) - mgx_3,$$

subject to the non-holonomic constraints (7), (8) and (9). For a standard Foucault pendulum only small oscillations are important, therefore $\dot{x}_3 \simeq 0$ and, from the holonomic constraint we have

$$x_3 = \sqrt{\ell - x_1^2 - \delta x_1^2} \simeq \ell - \frac{1}{2\ell}(\delta x_1^2 + x_2^2),$$

so that the Lagrangian reduces to

$$L = \frac{m}{2}(\dot{x}_1^2 + \dot{x}_2^2) - \frac{mg\delta}{2\ell}x_1^2 - \frac{mg}{2\ell}x_2^2$$

together with the non-holonomic constraint

$$\dot{\xi}_3 = x_1\dot{x}_2 - x_2\dot{x}_1. \tag{10}$$

On the three-dimensional manifold with local coordinates $q = (x_1.x_2, \xi_3)$, the kernel of the constraint (10) can be encoded in the distribution generated by the vector fields $X_1 = \partial_{x_1} - x_2\partial_{\xi_3}$ and $X_2 = \partial_{x_2} + x_1\partial_{\xi_3}$. In consequence, by taking the control parameter as the velocities $u = (u_1, u_2) = (\dot{x}_1, \dot{x}_2)$, the model for the Foucault pendulum can be formulated as the optimal control problem consisting in the minimization of the functional

$$\int c(x,u)dt,$$

with

$$c(x,u) = \frac{m}{2}(u_1^2 + u_2^2) - \frac{m\omega_1}{2}x_1^2 - \frac{m\omega_2}{2}x_2^2$$

and $\omega_1 = \sqrt{g\delta/\ell}, \omega_0 = \sqrt{g/\ell}$, among the admissible solutions of the control system

$$\frac{dq}{dt} = u_1X_1(q) + u_2X_2(q),$$

The distribution $\Delta = \{X_1, X_2\}$ is bracket generating, regular and generates a three dimensional step-2 nilpotent Lie algebra with the only non-zero brackets $[X_1, X_2] = X_3$, in fact we have a Lie algebra isomorphic to the Heisenberg Lie algebra, and the manifold $\mathcal{M}$ is the Heisenberg group.

We consider the corresponding Hamiltonians (momenta) $H_i's$ associated to the vector fields $X_i's$. The coordinates on the cotangent bundle are $(x_1, x_2, H_1, H_2)$ and the algebra for the $H_i$' is enlarged, see for example [Abraham and Marsden, 1987], according to

$$\{x_i, x_j\} = 0, \quad \{x_i, H_j\} = X_j(x_i).$$

The commuting relations for the step-2 nilpotent Lie-Poisson algebra generated by the Hamiltonians and the coordinates functions is summarized in the following table

| $\{\cdot,\cdot\}$ | $H_1$ | $H_2$ | $x_1$ | $x_2$ |
|---|---|---|---|---|
| $H_1$ | 0 | $H_3$ | $-1$ | 0 |
| $H_2$ | $-H_3$ | 0 | 0 | $-1$ |
| $x_1$ | 1 | 0 | 0 | 0 |
| $x_2$ | 0 | 1 | 0 | 0 |

Table 1

The control dependent Hamiltonian is written as follows

$$\mathcal{H}_{\mathbf{u}} = -c(x,u) + u_1H_1 + u_2H_2. \tag{11}$$

The maximality condition of the PMP readily implies that along extrema $u_i = H_i$, therefore the system Hamiltonian becomes quadratic

$$\mathcal{H} = \frac{1}{2m}(H_1^2 + H_2^2) + \frac{m\omega_1}{2}x_1^2 + \frac{m\omega_2}{2}x_2^2.$$

The differential system for the adjoint variable is written by Poisson bracketing as follows:

$$\begin{aligned}
\dot{H}_1 &= \{H_1, \mathcal{H}\} = H_2H_3 - m\omega_1x_1,\\
\dot{H}_2 &= \{H_2, \mathcal{H}\} = -H_1H_3 - m\omega_0x_2,\\
\dot{H}_3 &= \{H_3, \mathcal{H}\} = 0,
\end{aligned}$$

from where we can perform a straightforward integration process.

## 5 Foucault Pendulum and the Hopf Fibration

As it is shown in our previous work [Anzaldo-Meneses and Monroy-Pérez, 2009] the solution can be better written by introducing the complex variable $u = x_1 + ix_2$, from where $\dot{\xi}_3 = \mathrm{Im}\,(u\dot{u}^*)$ and $\ddot{u} = -i\frac{2\lambda_3}{m}\dot{u} - \frac{g}{\ell}u$, from where it follows that

$$\begin{aligned}
u &= e^{-i\tilde{\omega}\,t}(A_+e^{i\tilde{\omega}_0\,t} + A_-e^{-i\tilde{\omega}_0\,t}),\\
\dot{u} &= i\,e^{-i\tilde{\omega}\,t}(\alpha_+A_+e^{i\tilde{\omega}_0\,t} + \alpha_-A_-e^{-i\tilde{\omega}_0\,t}),\\
\xi_3 &= -(\alpha_+|A_+|^2 + \alpha_-|A_-|^2)\,t\\
&\quad -2\Re\Big(A_+A_-^*\,(e^{2i\,\tilde{\omega}_0\,t} - 1)\Big).
\end{aligned}$$

For the first two relations, this is a rotation given by the slow mode, with frequency $\tilde{\omega}$, of the fast mode motion, with frequency $\tilde{\omega}_0$. Therefore, the trajectory in base space performs a precession with frequency $\omega\sin(\alpha)$, whereas $\xi_3$ increases by the same amount after $2\pi/\tilde{\omega}_0$ where $\tilde{\omega}_0 = \sqrt{\tilde{\omega}^2 + \omega_0^2}$, $\omega_0 = \sqrt{g/\ell}$ and $\tilde{\omega} = \lambda_3/m$. Here, $\tilde{\omega}$ is equal to the rotation angular speed $\omega$ times the sinus of the geographical latitude, and the $A_\pm$ depends on the initial conditions. The conservation of energy reads now as follows

$$2H/m = |\dot{u}|^2 + \omega_0^2|u|^2. \tag{12}$$

For instance, for the original Foucault experimental setting one has, $x_1(0) = R\cos\beta$, $x_2(0) = R\sin\beta$, with $\beta \in (0, 2\pi)$, and $\dot{x}_1(0) = 0$ and $\dot{x}_2(0) = 0$, the trajectories are written as follows:

$$\begin{aligned}
x_1 &= R\cos(\tilde{\omega}t - \beta)\cos(\tilde{\omega}_0\,t)\\
&\quad + \frac{R\tilde{\omega}}{\tilde{\omega}_0}\sin(\tilde{\omega}t - \beta)\sin(\tilde{\omega}_0\,t),\\
x_2 &= -R\sin(\tilde{\omega}t - \beta)\cos(\tilde{\omega}_0\,t)\\
&\quad + \frac{R\tilde{\omega}}{\tilde{\omega}_0}\cos(\tilde{\omega}t - \beta)\sin(\tilde{\omega}_0\,t),\\
\xi_3 &= \frac{R^2\,\tilde{\omega}\,\omega_0^2}{\tilde{\omega}_0^2}\left(\frac{t}{2} - \frac{\sin(2\tilde{\omega}_0\,t)}{4\tilde{\omega}_0}\right).
\end{aligned}$$

Observe that the expressions for $x_1$ and $x_2$ are a rotation by an angle $\alpha = \tilde{\omega}t - \beta$ of the ellipse given by the vector

$$(R\cos(\tilde{\omega}_0\, t), \frac{R\tilde{\omega}}{\tilde{\omega}_0}\sin(\tilde{\omega}_0\, t)).$$

This vector has initial value $(R, 0)$ and takes the same value at times $t_k = \pi\, k/\tilde{\omega}_0$, for $k$ integer. Since $\tilde{\omega} < \tilde{\omega}_0$, the nearest approach to the origin is at distance $R\tilde{\omega}/\tilde{\omega}_0$. The curves in base space are hypocycloids.

We establish now a connection of these solutions with the well know Hopf fibration see for instance [Naber, 2000] and [Urbantke, 2003]. We consider only the symmetric pendulum.

We start by introducing the two complex variables $z_1 = \omega_0\sqrt{m/2H}\, u$ and $z_2 = \sqrt{m/2H}\, \dot{u}$, the dynamics develops on a unit 3-sphere $S_3$ given by the conservation of energy (12) that now is written as

$$|z_1|^2 + |z_2|^2 = 1.$$

Now, by means of Hopf map $\pi : S_3 \to \mathbb{CP}^1 = S_2$, there is a two unit sphere $S_2$ described by the unit vector $\hat{n} = (n_1, n_2, n_3)$ with components $n_1 = 2\mathrm{Re}(z_1 z_2^*)$, $n_2 = 2\mathrm{Im}(z_1 z_2^*)$ and $n_3 = |z_1|^2 - |z_2|^2$, satisfying

$$n_1^2 + n_2^2 + n_3^2 = 1.$$

This surface is known as *Bloch sphere* in the study of two level systems, of nuclear magnetic resonance, nonlinear optics and quantum computing. Observe that the sets of points $z_0 z_1$ and $z_0 z_2$ for $|z_0| = 1$ are circles through $z_1$ respectively through $z_2$ and are mapped to the same point on $S_2$.

The fiber bundle structure is given by $S_1 \hookrightarrow S_3 \xrightarrow{\pi} S_2$ where $S_3$ is the total space, $S_2$ the base space, $S_1$ the fiber space and $\pi$ the projection. In our problem to multiply $z_1$, respectively $z_2$, by a unit complex number is equivalent to rotate the plane $\{x_1, x_2\}$.

Since the solution is a rotation by an angle $\tilde{\omega}t$ of an ellipse parameterized by an angle $\tilde{\omega}_0 t$, we conclude that, all arcs of trajectories in base space, which can be obtained by a rotation from a given one, are mapped to the same curve on $S_2$ by the Hopf map. The resulting curve will be thus the same for all *equivalent* arcs. The Bloch vector $\hat{n}$ satisfies

$$\frac{d\hat{n}}{dt} = \vec{\Omega} \times \hat{n}, \tag{13}$$

with constant angular velocity $\vec{\Omega} = (0,\, -2\omega_0,\, 2\tilde{\omega})$. The canonical angular momentum conservation leads to the planes

$$-\omega_0 n_2 + \tilde{\omega} n_3 = \frac{1}{2}\vec{\Omega}\cdot\hat{n} = \frac{\omega_0^2\, L_z}{H} - \tilde{\omega}.$$

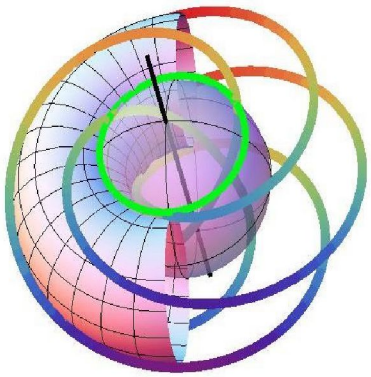

Figure 2. Villarceau circles and the Bloch sphere.

They are at a distance $(\omega_0^2 L_z - H\tilde{\omega})/(H\tilde{\omega}_0)$ from the origin, their normal unit vectors are $(0, -\omega_0/\tilde{\omega}_0, \tilde{\omega}/\tilde{\omega}_0) = \vec{\Omega}/\Omega$ and the intersections of these planes with $S_2$ are of course circles. In the case for which $H = mR^2\omega_0^2/2$ we have

$$\hat{n} = (-\frac{\omega_0}{\tilde{\omega}_0}\sin(2\tilde{\omega}_0 t), \frac{\omega_0(-\tilde{\omega} + \tilde{\omega}\cos(2\tilde{\omega}_0\, t))}{\tilde{\omega}_0^2}, \frac{\tilde{\omega}^2 + \omega_0^2\cos(2\tilde{\omega}_0\, t)}{\tilde{\omega}_0^2}).$$

The two halves of the spheres are foliated by circles independent of the initial position $R$ or the energy. The circles on one half are for $\tilde{\omega}/\omega_0 > 0$ and on the other half for $\tilde{\omega}/\omega_0 < 0$. All circles pass through the north pole. The isolated north pole also corresponds to the limit cases where the ratio of the frequencies is $\pm$ infinity, associated to the Heisenberg flywheel or a charged particle in a perpendicular static magnetic field. When $\tilde{\omega}/\omega_0 = 0$ the circles become a meridian that corresponds to a two dimensional harmonic oscillator. For $\tilde{\omega}/\omega_0 = \pm 1$ two circles connect the north pole with the equator. Finally, each circle corresponds to a single curve arch in the base space $\{x_1, x_2\}$ trajectory traversed in half a period. For the general case $H = mx_0^2\omega_0^2/2 + mv_0^2/2$ and $L_z = mx_0 v_0\sin(\beta) + m\tilde{\omega}x_0^2$, see Figure 2.

The components of the normal vector are

$$\begin{aligned}
n_1 &= \frac{m\omega_0}{2H\tilde{\omega}_0}(2\tilde{\omega}_0 v_0 x_0\cos(\beta)\cos(2\tilde{\omega}_0 t) \\
&\quad + [v_0^2 - \omega_0^2 x_0^2 + 2\tilde{\omega}v_0 x_0\sin(\beta)]\sin(2\tilde{\omega}_0 t)), \\
n_2 &= \frac{m\omega_0}{2H\tilde{\omega}_0^2}(\tilde{\omega}v_0^2 - \tilde{\omega}\omega_0^2 x_0^2 - 2\omega_0^2 v_0 x_0\sin(\beta) \\
&\quad - \tilde{\omega}\cos(2\tilde{\omega}_0 t)[v_0^2 - \omega_0^2 x_0^2 + 2\tilde{\omega}v_0 x_0\sin(\beta)] \\
&\quad + 2\tilde{\omega}\tilde{\omega}_0 v_0 x_0\cos(\beta)\sin(2\tilde{\omega}_0 t)) \\
n_3 &= \frac{m}{2H\tilde{\omega}_0^2}\Big(-\tilde{\omega}^2 v_0^2 + \omega_0^2\tilde{\omega}^2 x_0^2 + 2\omega_0^2\tilde{\omega}v_0 x_0\sin(\beta) \\
&\quad - \omega_0^2\cos(2\tilde{\omega}_0 t)[v_0^2 - \omega_0^2 x_0^2 + 2\tilde{\omega}v_0 x_0\sin(\beta)] \\
&\quad + 2\omega_0^2\tilde{\omega}_0 v_0 x_0\cos(\beta)\sin(2\tilde{\omega}_0 t)).
\end{aligned}$$

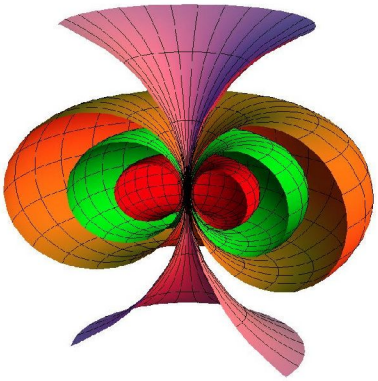

Figure 3. Nested tori and the Hopf fibration.

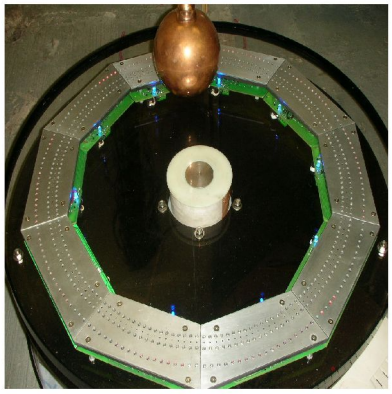

Figure 4. The Foucault Pendulum at UAM-A.

Again, the conservation of the canonical angular momentum leads to circular trajectories around the vector $\vec{\Omega}$.

For $\tilde{\omega} = 0$, uncoupled harmonic oscillator, the coordinate $n_2$ is constant and the corresponding limit circle is perpendicular to the $\{n_1, n_2\}$ plane and separates the sphere in two unequal parts in general. The limit case $\omega_0 = 0$ is the south pole for $v_0 \neq 0$, since then $n_3 = -1$, and the north pole for $v_0 = 0$ and $x_0 \neq 0$ which lead to $n_3 = 1$.

Perform now a rotation such that the angular velocity $\vec{\Omega}$ coincides with the $n_3$ axis, i.e., introduce the coordinates $n_1' = n_1, n_2' = \tilde{\omega} n_2/\tilde{\omega}_0 + \omega_0 n_3/\tilde{\omega}_0$ and $n_3' = -\omega_0\, n_2/\tilde{\omega}_0 + \tilde{\omega} n_3/\tilde{\omega}_0$. More explicitly

$$n_2' = \frac{m\omega_0}{2H\tilde{\omega}_0}(-[v_0^2 - \omega_0^2 x_0^2 + 2\tilde{\omega} v_0 x_0 \sin(\beta)]\cos(2\tilde{\omega}_0 t) + 2\tilde{\omega}_0 v_0 x_0 \cos(\beta)\sin(2\tilde{\omega}_0 t)).$$

The coordinate $n_3'$ is the constant $(\omega_0^2 L_z - \tilde{\omega} H)/(H\tilde{\omega}_0)$ and $(n_1', n_2')$ describes a circle centered on the $n_3'$ axis.

Further geometrical analysis shall be carried out somewhere else for exploiting the richness of the Hopf fibration in the same spirit of the aforementioned reference of H.K. Urbantke. Figure 3 illustrates the Hopf fibration aroun the bloch sphere

## 6 The Foucault Pendulum at UAM-Azcapotzalco

One of the motivations for studying theoretical aspects of the Foucault pendulum was the involvement of the authors in the project of installation of a real Foucault pendulum at the UAM-Azcapotzalco in México City. The project is now at the level of a prototype design that we shall briefly describe it.

### 6.1 Physical Characteristics

It consist of a perfect 10 kilograms bronze (SAE 65) sphere with a central cilindrical axis of 1in of diameter of stainless steel (SW 10), perfectly coupled to the sphere. This ferromagnetic composition allows the action of electromagnetic devices. The sphere is suspended by a iron cable of seven threads of type $(1 \times 7 + 0)$, see Figure 3.

The pendulum is initialized as in the original experiment from rest and is energized by mean of an electromagnetic impulse on the bottom by means of a coil that energizes the pendulum on a regular basis. The electromagnetic force was calculated by means of a COMSOL Multiphysics 3.5's simulation for a permanent oscillation of $5^\circ$, see Table 2.

| $1^\circ$ | $2^\circ$ | $3^\circ$ | $4^\circ$ | $5^\circ$ |
|---|---|---|---|---|
| -1.1 E08 | 4.2 E07 | 1.3 E07 | -9.8 E10 | 4.2 E10 |
| 7.4 E06 | -6.8 E06 | -3.9 E05 | -1.9 E06 | -2.9. E07 |
| -5.0 E04 | -5.4 E04 | -1.2 E05 | -2.8 E07 | -5.8 E08 |
| 5.0 E04 | 5.4 E04 | 4.1 E05 | 2.0 E06 | 2.9 E07 |

Table 2. Estimation of the electromagnetic impulse.

### 6.2 The Control and Vision System

It consist of three fundamental parts, namely, a three rings circular configuration of eight independent modules of sensors. An interactive mechanism with a central controller of each module and an we cam. The permanent communication of the modules determines a a closed loop scheme where feedback is generated by infrared presence sensors that triggers the electromagnetic impulse within a determined threshold, see figure 3. The web cam has a fix IP and interfaces with the central controller for keeping track of the movement, for generating data regarding position, velocity and acceleration, as well as database of images that can be used for image reconstruction experiments.

## 7 Conclusion and Research Perspectives

We formulate the classical Foucault pendulum in the framework of geometric optimal control theory, the small oscillation considerations allows to reduce the state manifold to the three dimensional Heisenberg group. The Pontryagin Maximum Principle yields the optimal controls that allow to write explicitly the solutions. With these expressions at hand we establish

an intriguing connection with the well known Hopf fibration, that open an interesting line of theoretical research. At the end we describe the main features of a prototype of a real Foucault pendulum in process of being installed at the UAM-Azcapotzalco in México City, the apparatus includes a closed loop feedback scheme as well as a monitoring vision system.

**References**


Abraham, R., and Marsden, J.E. (1987) *Foundations of Mechanics*, Addison-Wesley.

Agrachev, A., and Sachkov, Y.L. (2004) *Control Theory from the Geometric Viewpoint. Encyclopaedia of Mathematical Sciences. 87, Control Theory and Optimization, II.* Springer-Verlag, Berlin.

Anzaldo-Meneses, A., and Monroy-Pérez, F. (2009) *Sub-Riemannian Approach for the Foucault Pendulum*, PHYSCON 2009, Catania, Italy.

Anzaldo-Menenses, A., and Monroy-Pérez, F. (2010) *J. math. Phys.*, **51**, pp. 082703.

Brockett, R.W. (1972) System theory on group manifolds and coset spaces. *SIAM J. Control*, **10**.

Bullo, F., and Lewis, A.D. (2004) *Geometric Control of Mechanical Systems. Texts in Applied Mathematics*, Springer.

Calin, O., and Chang, D.Ch. *Sub-Riemannian Geometry General Theory and Examples, Encyclopedia of Mathematics and its Applications. 126*, Cambridge University Press.

Giaquinta, M., and Hildebrandt, S. (1996) *Calculus of Variations. I. The Lagrangian Formalism. Grundlehren der Mathematischen Wissenschaften [Fundamental Principles of Mathematical Sciences]*, 310. Springer-Verlag, Berlin.

Jurdjevic, V. (1997) *Geometric Control Theory. Cambridge Studies in Advanced Mathematics*. 51, Cambridge University Press.

Jurdjevic, V., and Sussmann, H.J. (1972) Control systems on Lie groups. *J. Differential Equations*, **12**.

Lobry, C. (1970) Contrôlabilité des systèmes non linéaires. *SIAM J. Control*, **8**.

Montgomery, R. (2002) *A Tour of Subriemannian Geometries, Their Geodesics and Applications. Mathematical Surveys and Monographs, 91*, American Mathematical Society.

Murray, R., Zexiang, L., and Sastry, S.S. (1994) *A Mathematical Introduction to Robotic Manipulation*, CRC Press.

Naber, G.L. (2000) *Topology, Geometry and Gauge Fields, Interactions. Applied Mathematical Sciences, 141*, Springer-Verlag, New-York.

Pontryagin, L.S., Boltyanskii, V.G., Gamkrelidze, R.V., and Mishchenko E.F. (1962) *The Mathematical Theory of Optimal Processes* ed. by L.W. Neustadt Interscience Publishers. John Wiley & Sons, Inc. New York-London.

Vershik, A.M., and Gershkovich, V.Ya. (1991) Nonholonomic dynamical systems, geometry of distributions and variational problems. *Encyclopaedia of Mathematical Sciences, 16, Dynamical systems VII*, V.I. Arnold and S.P. Novikov eds., Springer-Verlag.

Urbantke, H.K. (2003) The Hopf fibration — seven times in physics. *Journal of Geometry and Physics*, **46**, pp. 125–150.

Young, L.C. (1969) *Lectures on the Calculus of Variations and Optimal Control*, Philadelphia, Saunders.